THE ARCHIVE OF MECHANICAL ENGINEERING

Vol. LI 2004 Number 3

Key words: *aerospace aluminium alloy, fatigue crack growth rate, programmed loading, fractographic analysis*

*DOROTA KOCAŃDA**), *STANISŁAW KOCAŃDA**), *JANUSZ TORZEWSKI**)

RECONSTRUCTION OF FATIGUE CRACK GROWTH RATE FOR 2024-T3 ALUMINIUM ALLOY SHEET ON THE BASIS OF FRACTOGRAPHIC ANALYSIS

Fatigue crack growth for 2024-T3 Alclad aluminium alloy sheet being subjected to two load programs: a constant stress amplitude cyclic tension (R=0.1) (CA) and a variable amplitude tension with either a single or multiple overloads (OVL) periodically repeated is analysed in the paper. The latter load program corresponds to a simple flight simulation spectrum of wing structure of civil aircraft. The investigation was developed in order to learn about interaction between the applied load and formation of fatigue striations. Experimental results of surface crack growth rate provided by optical observations were compared with the rate determined on the basis of microfracture analysis. Good correspondence found under CA loading between the surface growth rate and the growth rate in the sheet depth means that the direction of specimen's cutting does not change essentially the crack growth behaviour. In the case of second loading (OVL) this factor influences the crack growth behaviour. Microfracture analysis revealed either retardation and acceleration of crack growth rate under OLV loading. This behaviour of growth rate results from a plastic zone formed in the front of crack tip and a crack closure effect.

1. Introduction

Feasibility of reconstruction of fatigue crack growth in a component on the basis of fractographic analysis is well known and practically used for many years. For this goal, characteristic features of fracture surface of the component, namely macroscopic growth lines as well as the fatigue striations in relation to the applied load are analysed. However, in many cases either of

*) *Military University of Technology, Faculty of Mechanics, Kaliskiego 2, 00-908 Warsaw, Poland; E-mail: d.kocanda@wme.wat.edu.pl*

loads or the tested materials, the fatigue striations may be invisible on the fracture surface. Furthermore, the relation one cycle-one striation may be satisfied only in a middle part of the crack growth curve. Many researches carried out on this problem indicate that the growth rate estimated from the striations spacing is higher in the initial stage of crack growth, and lower in the final stage of crack growth, than the rate determined by other methods [1]. Of course, it is not the rule. For instance, mutual correspondence between the crack growth rates was observed for 2024-T3 aluminium alloy at the constant amplitude loading in whole range of crack growth [2]. In the mentioned paper [2] a short overview of the works published in the period 1996–1999 was included. For this reason, in the present work only new successive researches concerning load-time history reconstruction for aluminium alloys by means of fractographic analysis will be mentioned.

The work by Wanhill [3] points out that the micrographs taken from the fracture surfaces of 2024-T3 test samples conducted under simulated spectrum load correctly imaged the load history. Furthermore, the features of fracture surface were similar to these related to a real structure under service loading. The bands lain between visible fatigue striations were corresponded to 5000 flights. Spectrum loading was accurately marked on the fracture surface by the systems of fatigue striations in aerospace aluminium alloy AA7010 [4]. Experimentally determined crack growth rate for A2017-T3 aluminium alloy under three-step varying load was compared with the rate estimated from the striations spacing [5]. Pretty good agreement between these rates was achieved for two load sequences. In the case of third load program the results were completely divergent. Microfracture analysis was employed in order to investigate the influence of applied load sequences on crack growth rates for 2024 alloy after different surface treatments [6]. The results of this experiment permitted unique discrimination of the interaction effects between applied load and the relative changes in formation of fatigue striations. The effect of hydrogen environment embrittlement on fatigue crack growth behaviour in six aerospace aluminium alloys, among them also in 2024-T3 alloy, was the subject of [7]. Extensive investigations in this field were conducted in the conditions of time-dependent hydrogen exposure as well as time-dependent cyclic deformation in gaseous, aqueous environments and in ultra-high vaccum. SEM micrograph derived from a transition zone revealed in 2024-T3 alloy a quasi-cleavage mechanism of cracking in vaccum, and afterwards the occurrence of fatigue striations when the cracking process was developed on in moist air. Fatigue striations were invisible in 7075-T3 alloy plates with semi-elliptical notches under constant amplitude tension [8]. However, the presence of fatigue striations was confirmed after inserting the overloads in the basic load spectrum.

The importance of fractography supporting the analysis of failure case of real structures has been pointed out by J. Schijve either in his recently published book [9] or at the ECF-14 conference in Cracow [10]. Special needs that concern fatigue damage of aircraft components persist also the researches to investigate fatigue crack propagation in aerospace aluminium alloys under different types of load-time histories. These reasons require special skills for finding the correlation between the images of fracture surface and the accumulated fatigue damage due to the applied load. The relation one cycle-one striation was examined in [9] in order to determine the rates of crack growth for different types of simulated service loading and then exemplified in the diagrams of growth rates versus number of cycles. However, it should be mentioned that the references devoted to this problem provide both positive and negative opinions on the fractography ability when reconstructing the load-time history of a failed component. Surprising results were obtained in [11] when investigating *in situ* small crack behaviour in 2024-T351 polycrystalline alloy under tension and under bending. The analysis of fracture surface proved a plastic mechanism of cracking. However, fatigue striations were not evident on the surface.

Load interaction effects on fatigue crack growth response when imposing a single or multiple overloads are widely reported in the references. For load histories containing overloads, the evidence of fatigue striations on fracture surface depends on particular combination of load parameters and material. When relating the crack growth to the load parameters, one needs to take into account the number and the frequency of overloads imposed during basic loading (BL) as well as the ratio of the overload stress OLR defined below. However, it can happen that the multiple overloads which intersperse the baseline cycles do not mark the striations on fracture surface. This case is often observed in aluminium alloys and is reported in the studies mentioned below. A negligible effect of overloads on the crack growth rate appeared in aluminium alloys such as 2024-T3 [12], 7075 and 8090 [13] under aircraft service spectrum as well as in another seven aerospace aluminium alloys [14]. This fact was confirmed by the plots of crack growth rate also for 2524-T3 Alclad aluminium sheets and in titanium alloys [15] under the Embraer simulated service utilisation. To the contrary, stronger interaction effects on crack growth behaviour appeared in 2024-T3 when a single overload was applied and consequently multiplied until failure [12]. The mentioned results were also confirmed in our research developed for 2024-T3 aluminium alloy.

Therefore, there is a considerable interest in evaluating the capacity of the models for fatigue crack growth prediction. To this end, a research program on fatigue crack growth behaviour has been developed for thin 2024 sheets

after two different heat treatments T3 and T2. The sheets were subjected to variable amplitude sequences typical to helicopter utilisation to support analytical and numerical modelling of crack growth in lower wing skin [16]. It was found that 2024-T2 specimens exhibited slightly longer crack propagation lives as compared to 2024-T3 Alclad specimens. The accuracy and the reliability of the prediction models commonly used by FASTRAN, NASGRO, CORPUS and AFGROW were tested to evaluate the plots of crack length versus number of cycles as well as the distribution of the ratio of the number of cycles measured in the experimental test over the calculated ones, for a given crack growth intervals. The results of comparisons showed big discrepancies between these plots. The retardation and acceleration effects due to the imposed overloads were clearly marked in the experimental plots. The trends in crack growth behaviour were illustrated only by three predicted plots. The worst results were derived by AFGROW. Crack growth analysis for 7075-T6 aluminium alloy under service loading with the help of identical numerical programs as mentioned in [16] was the subject of the work [17].

A wide review of fatigue crack growth behaviour for the metallic materials, among them also for aluminium alloys, under both simple and complex load sequences of variable amplitude as well as the presentation of fatigue crack growth prediction models can be found in the monograph [18].

The present work derives the results of fatigue crack growth response in 2024-T3 aluminium alloy to the application of a simple load sequence interspersed by overloads. This kind of load sequence is employed when simulating the fatigue behaviour of aeronautical alloys. The problem of reconstruction of the fatigue crack growth on the basis of microfracture analysis is also considered here.

2. Material. Experimental procedure

The material used for testing was 2024-T3 Alclad aluminium alloy sheet of 3 mm thickness, which was manufactured by French factory of Pechiney-Rhenalu. Clad layer thickness was 0.120 mm. The specimens, cut from the sheet, had the size of 400 mm length and 100 mm width. In order to facilitate comparison of fatigue properties with respect to rolling direction, the specimens were cut from the sheet in three directions: parallel (LT), transverse (TL) and under 45 degrees (45) due to rolling. Three series of specimens (LT, TL, 45) under examinations showed the scatters of static mechanical properties in the following ranges: ultimate tensile stress (R_m) 447–466 MPa, yield stress (R_{02}) 303–335 MPa, elongation (A) 21–24%. The highest values of these properties were found for LT specimens. However, in

those specimens loaded in CA cyclic tension fatigue crack growth rates were found to be independent on the cutting direction. For crack propagation studies, the specimens were provided with a central notch consisting of a through-thickness hole of 5 mm diameter, through-thickness saw cut of 2.5 mm length and pre-cracking of 2.5 mm length on each side of the hole. According with the fracture mechanics notation, the initial crack length $2l$ was equalled to the length from tip to tip of pre-cracking. In our case, $2l$ = 15 mm. Fatigue tests were carried out in cyclic tension under two load programs. First program was a constant-amplitude stress loading (CA) with the stresses altered in the range from σ_{min} = 5 MPa to σ_{max} = 80 MPa (R = 0.0625) with a frequency of 2 Hz. Second program (OVL) contained a load sequence of 211 cycles with few overloads, as shown in Fig. 1, which was periodically repeated until failure with a frequency of 2 Hz. The basic constant-amplitude load (CA), similar the first load program, was interspersed by 10 uploads, and then by a single similar upload followed by 100 basic cycles. Successive 10 overloads were also preceded by 100 basic cycles. Maximum stress at the overload was σ_{max} = 100 MPa and the overload rate OLR = 1.266. The overload rate OLR was defined as $OLR = (K_{OL} - K_{min,\,BL}) / (\Delta K_{BL})$ where K_{OL}, $K_{min,\,BL}$ mean stress intensity factors at the overload and at the minimum stress in basic cycles, respectively. The symbol $\Delta K_{BL} = (K_{max,\,BL} - K_{min,\,BL})$ defines the range of stress intensity factor calculated for the baseline cycles.

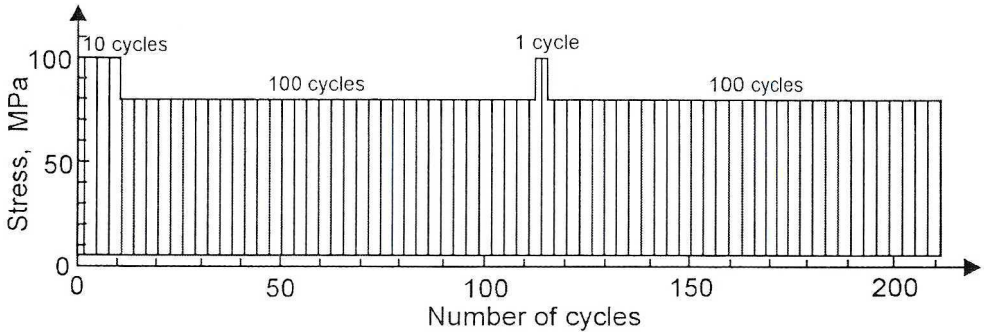

Fig. 1. Load sequence with overloads

The loading program (Fig. 1) proposed by J. Schijve from the National Aeronautical Laboratory in Delft (Netherlands) was employed for crack propagation test as a simple flight simulation load of wing structure of civil aircraft. Surface crack growth process was detected continuously without test interruption by using a high-speed camera equipped with a disk recording. Then, the stored data of the crack tip positions were downloaded and analysed by a graphic program which allowed the measure of crack length to be

displayed on the computer screen. Fractographic analyses of fracture surface were carried out by means of the scanning (SEM) and transmission (TEM) electron microscopes. Prior to the TEM micro-observations, the replicas taken from the fracture surface were shadowed by platinum. Microscopic observations provided the details of mechanism of cracking, and made it possible to determine the correlation between the history of loading and the characteristic features of fracture surface. Crack growth rates determined from the striations spacing were compared with the rates of surface crack growth recorded by the camera.

3. Results and discussion

The analysis of fatigue crack growth response for 2024-T3 aluminium alloy due to the applied load spectrum will be provided separately for constant amplitude stress loading (CA) and programmed loading with overloads (OVL). It should be clearly emphasized that these considerations refer only to long crack behaviour.

4. Constant amplitude fatigue crack growth

Experimental fatigue crack growth rate courses as function of crack length and cycle ratio N_i/N_f (N_i – current number of cycles, N_f - number of cycles to failure) are shown in Figs. 2a and 2b, respectively. The courses in the diagrams are related to three series of tested specimens LT, TL and 45. The results obtained in the fatigue tests revealed that under CA loading the rates of crack growth in the examined specimens are practically independent on the direction of specimen's cutting due to rolling. The courses in Figs 2 showed a small scatter for the growth rates almost during the whole lives of the specimens. Though, certain scatters for these items have appeared in an initial stage of fatigue lives up to 0.3 N_i/N_f. It could indicate that mechanical properties of the material such as fracture toughness depend on the specimen's cutting. Similar small scatters can also be seen in Figs 2c and 2d when referring the courses of growth rate to the range of stress intensity factor ΔK (Fig. 2c) and to the range of the J_I – integral (mode I of cracking) in Fig. 2d. The ΔJ_I – integral was calculated according to the relationship given by Dowling [19]:

$$\Delta J_I = a \cdot \left(1.24 \frac{\Delta\sigma^2}{E} + 1.02 \frac{\Delta\sigma \cdot \Delta\varepsilon}{\sqrt{n'}} \right) \tag{1}$$

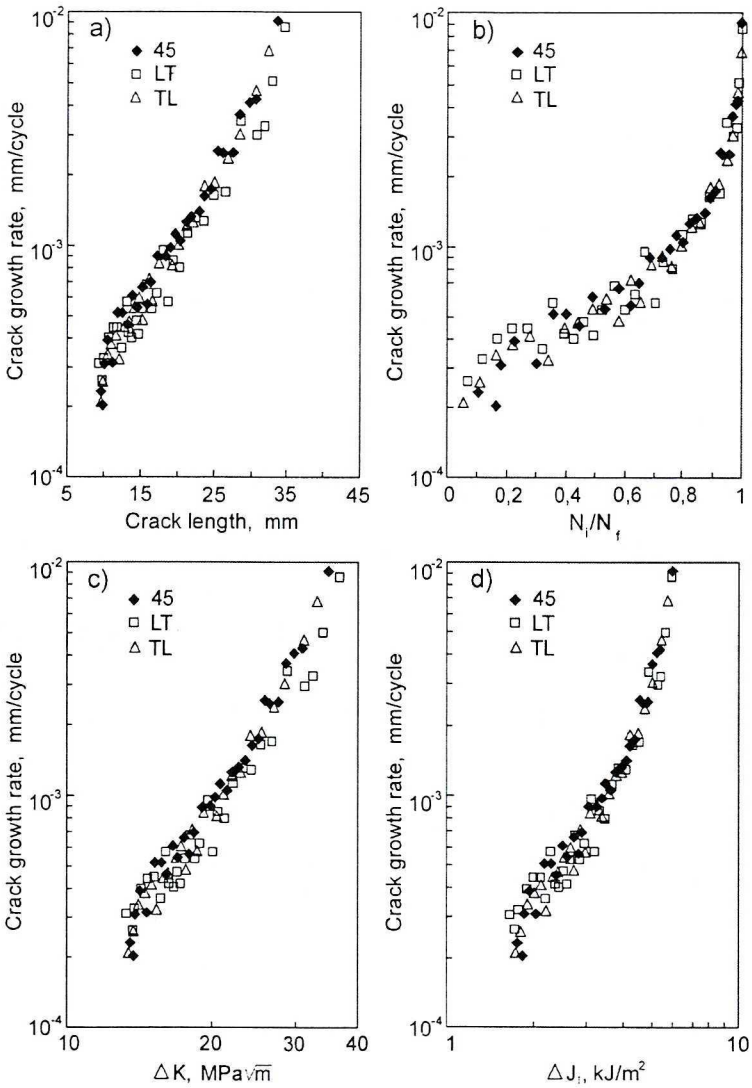

Fig. 2. Experimental courses of crack propagation rates for 2024-T3 aluminium alloy under constant amplitude tension (R = 0.1) against: (a) crack length, (b) cycle ratio N_i/N_f, (c) the range of stress intensity factor ΔK and (d) the range of J_I – integral

where a means crack length, $\Delta\sigma$ is the range of the applied stress, $\Delta\varepsilon$ is the strain range estimated from a cyclic stress-strain curve, n' is strain hardening exponent. For 2024-T3 aluminium alloy $n = 0.07$.

The resistance to fatigue crack growth of the used material under constant amplitude stress load is characterized by the Paris formula $da/dN = C \cdot (\Delta K)^m$. Least-squares fitting of the representation da/dN versus ΔK in double log scales in Fig. 2c to a straight line allows determination of the parameters such

as material constant $C = 3.203 \cdot 10^{-11}$ and the power exponent $m = 3.43$. Applying the same method for the data of Fig. 2d one derives the parameters $C_j = 5.129 \cdot 10^{-8}$ and $m_J = 2.52$ when the Paris formula is expressed by the function ΔJ_I.

The trends in crack growth rates reflected by the courses in Figs 2c and 2d correlate with the mechanism of cracking which was revealed by the TEM observations. Mainly a plastic mechanism in the form of fatigue striations was evident on the fracture surface of the specimens. Exemplary TEM micrographs in Fig. 3 with gradually increasing striations spacing along the crack

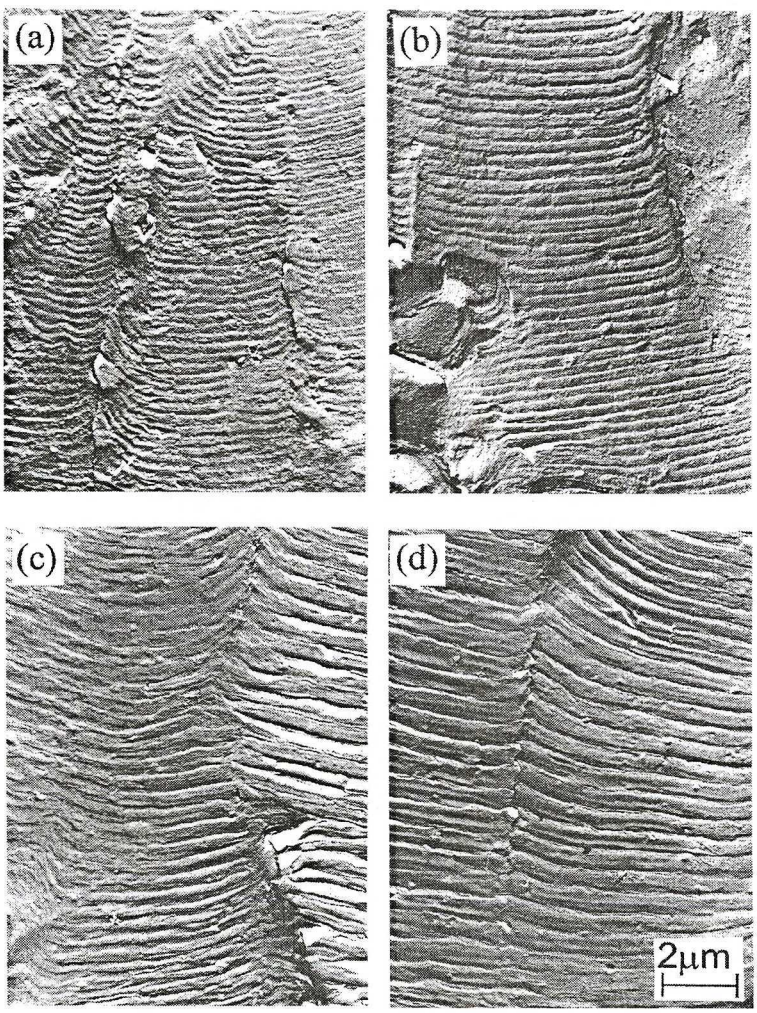

Fig. 3. TEM micrographs of the fracture surface with gradually increasing spacing between the fatigue striations along increased crack length; see the text for explanations

length were taken at an early stage of cracking process. Local crack growth rates in the relevant time instance were estimated for the proper spot on fracture surface by counting the spacing between the fatigue striations on the individual micrographs.

For example, the micrographs shown in Figs. 3 provide the following values of the rates: 0.275 μm/cycle (Fig. 3a), 0.350 μm/cycle (Fig. 3b), 0.550 μm/cycle (Fig. 3c) and 0.595 μm/cycle (Fig. 3d). Then, the local crack growth rates were compared with the rates determined by applying two other methods, namely optical one (OPT) and by means of scanning microscope (SEM). With respect to the method used for this goal, the sets of experimental data were differently marked in the comparative diagram in Fig. 4. Namely, black-filled diamonds refer to the optical surface crack length measures (OPT) in a relevant time instance. Open squares refer to the striations spacing measured with the help of the SEM microscope and finally open triangles relate to the measures done by using the TEM microscope. As it can be seen in Fig. 4, the correlation between the data can be assessed as quite good. The sets of experimental data lay in a small scatter band. It is the consequence of spacing between the striations regularly increasing in time what is presented in the TEM and SEM images.

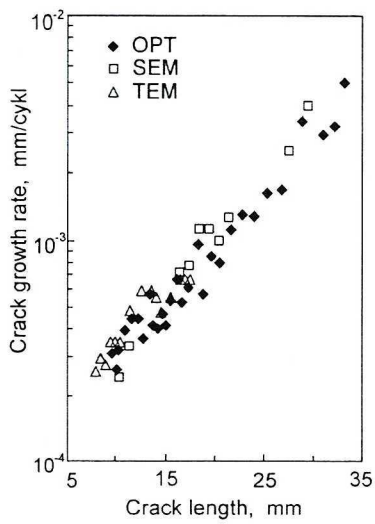

Fig. 4. Comparative diagram of crack growth rates determined by applying three different methods versus crack length; see explanation in the text

5. Fatigue crack growth under programmed loading

Fatigue crack growth behaviour of 2024-T3 under loading test with the overloads imposed on the baseline cycles as shown in Fig. 1 is presented in Fig. 5. Two experimental data sets of the crack growth rates associated with

crack advance along the specimen's surface under CA and OVL loadings are shown in the diagrams against: crack length (Fig. 5a) and cycle ratio N_i/N_f (Fig. 5b), respectively. The data marked by black diamonds refer to the CA test in tension. Second data set, marked by the open triangles, was obtained from the results of the OVL test. As it was expected, the overloads imposed in the constant stress amplitude load caused a significant retardation in crack growth rates.

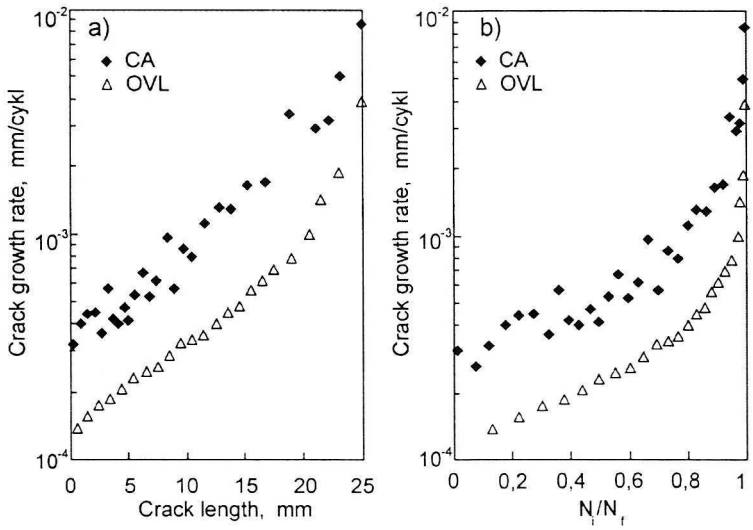

Fig. 5. Experimental courses of fatigue crack growth rates versus crack length (a) and cycle ratio N_i/N_f (b) under constant amplitude (CA) and programmed loading (OVL), respectively

However, the retardation and acceleration effects associated with a particular block of overloads are not clearly visible on the experimental plots in Fig. 5. Probably, it resulted from the methodology used when measuring crack length on the specimen surface. To the contrary, these effects of the overloads on fatigue crack growth response can be considered when one takes into account the TEM and SEM micrographs originating from the spots at different distances from the notch. Exemplary TEM micrograph in Fig. 6a shows a system of fatigue striations which corresponds to a half of the load sequence. On the upper image, from left to the right side, one can easily identify the band with 10 "thicker" striations originating from 10 applied overloads, then the band with 100 "tiny" striations corresponding to 100 basic cycles and a single "thicker" striation induced by one overload.

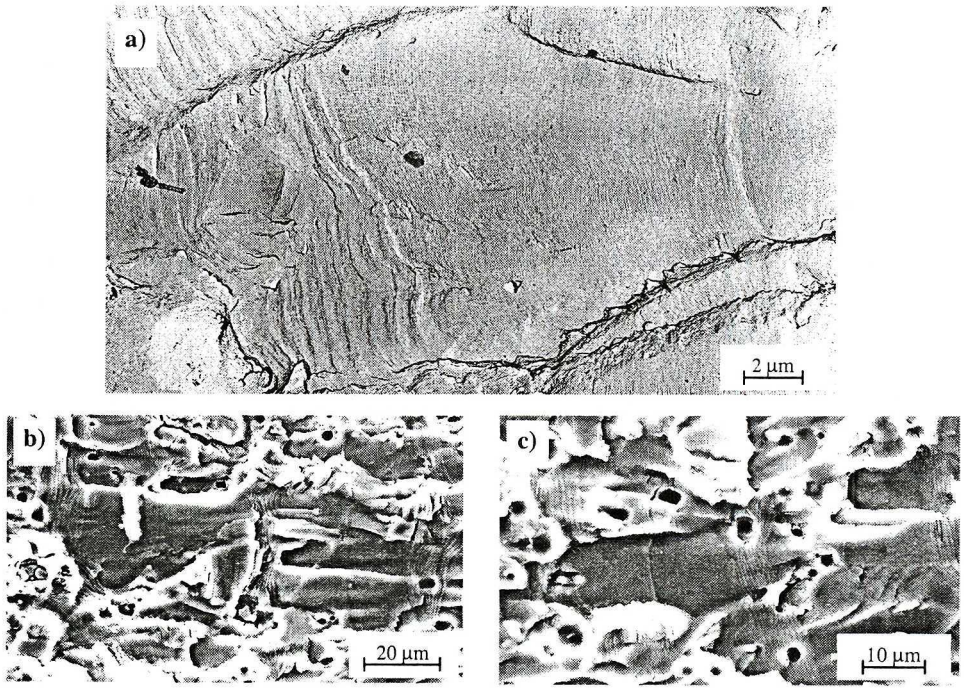

Fig. 6. The TEM (a) and SEM (b and c) micrographs illustrate the systems of fatigue striations on fracture surface under load sequence (OVL); see text for explanation

The successive band of 10 "thicker" striations is preceded by the band with 100 "tiny" striations. Let us note different spacing between the tiny striations inside this last band. Ten overloads give rise to severe retardation effect and very small striations spacing. The retardation effect becomes immediate after applying the overloads. When approaching the single thicker striation then the spacing between the striations gradually increases because of an acceleration in growth rate. Similar images of fatigue striation systems are shown in the SEM micrographs in Figs 6b and 6c. These are less readable, because of the presence of numerous brittle fracture areas in the matrix alloy, which are associated with randomly distributed precipitates.

The TEM and SEM micrographs allow us to reconstruct the fatigue crack growth rates in 2024-T3 alloy under a programmed loading. However, this reconstruction is possible only in a micro scale and is limited to a particular load sequence. The courses of local crack growth rate, affected by particular blocks of load cycles against crack length, are shown in Figs 7a and 7b. It should be explained that a block of load cycles comprises the whole load sequence as shown in Fig. 1. The length of crack, counted in micrometers, covers the spacing between two successive fatigue macro lines. Crack growth

rates were estimated on the basis of fatigue striations spacing and were referred to the particular blocks of loading. The marks used in the diagrams refer to the number of blocks that were passed in the fatigue test when measuring the crack length. The diagram in Fig. 7a depicts the changes of growth rates recorded in the range from 2 mm to 5 mm, whereas the diagram in Fig. 7b shows the results recorded in the range from 8 mm to 11 mm. The distance is counted from the end of the mechanical notch i.e. from the tip of the notch slit. As it can be seen on the left side of each diagram in Figs 7a and 7b ten overloads produce initially a high growth rate. However, the rate shows essentially a decreasing tendency and eventually a rapid drop almost of two orders of magnitude. Afterwards, the rate gradually increases in the period corresponded to 100 baseline cycles showing also certain periods of constant rates. Imposition of a single overload in the basic cycles results either in an immediate short jump of growth rate or its rapid drop of one order of magnitude. The load interaction leads to a delayed retardation of crack growth and then to its gradual rising in the period associated with the application of subsequent 100 basic cycles. The effect of crack growth retardation is associated with a plastic zone ahead of a crack tip, produced by the overloads, with the compressive stresses acted in this zone. These stresses temporarily close the tip of the crack. Further crack extension is possible when the crack tip leaves the plastic zone. As it is seen in the mentioned diagrams, multiple overloads give rise to a more severe crack growth rate retardation than a single overload. However, when comparing the plots in Fig. 7a and Fig. 7b, one can note a significant rise of crack growth rate with increasing number of load sequences passed in the test. For example, in Fig. 7a the growth rates were varying in the range from 10^{-3} to 10^{-5} mm/cycle after 140 blocks applied, whereas in Fig. 7b the rates were in the range from 10^{-2} to 10^{-5} mm/cycle after passing 224 blocks of cycles. In this time, the crack enlarged from 30 to 60 μm.

Crack growth behaviour in 2024-T3 Alclad aluminium alloy under programmed loading was analysed either on the surface or in the depth of the samples. As mentioned before, surface crack advance in time was recorded optically whereas the extension of crack depth was estimated on the basis of fractographic analysis with the help of SEM or TEM microscopes. Correlation between these growth rates for selected LT i TL specimens is shown in Fig. 8. Good correlation of the growth rates can be observed almost in the whole range of crack length under examination. The scatter for the crack growth rates was found only for TL specimen in an initial range of crack length when the growth rates were determined as the average local rate associated with the particular blocks of cycles. These discrepancies can result

from a difference between surface crack growth and the growth of crack depth particularly in TL specimen. However, this hypothesis could be confirmed if more specimens were examined.

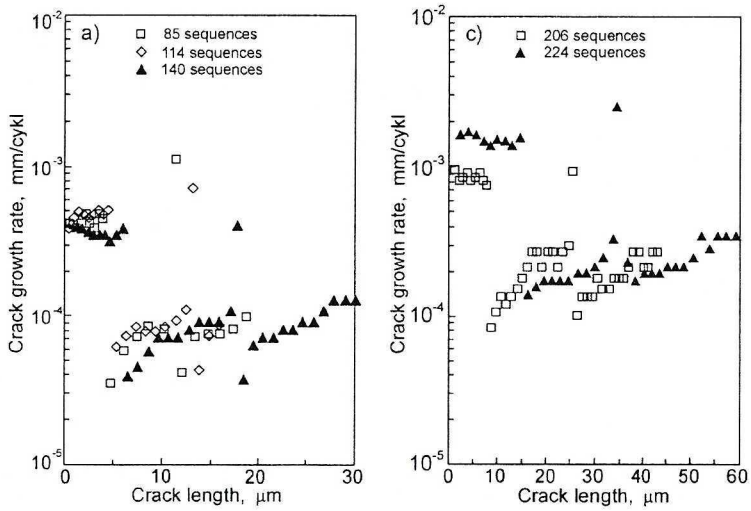

Fig. 7. The courses of crack growth rates against crack length within the range of 2–5 mm (a) and within the range of 8–11 mm (b) from the notch; see text for explanation

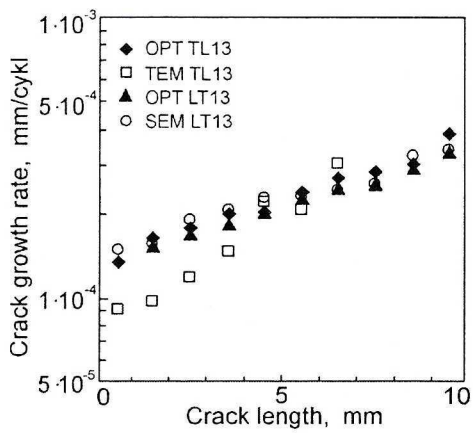

Fig. 8. Correlation between surface crack growth rate and the rate in the depth of the specimen versus crack length for 2024-T3 aluminium tested under programming loading; see text for explanation

6. Summary

Crack growth behaviour for 2024-T3 Alclad aluminium sheet was investigated under constant amplitude cyclic tension (CA) (R = 0.1) and under programmed loading with overloads (OVL). The research was developed in order to learn about the load influence on both long fatigue crack growth

response and formation of fatigue striations on the fracture surface. Surface crack growth was optically recorded, but the crack depth growth was analysed on the basis of striations spacing. Crack growth rate was estimated using a classical method, as well as on the basis of microfracture analysis with the help of scanning and transmission microscopes. Experimental and calculated results of growth rates were presented graphically on the diagrams. Microfracture analysis revealed a big variation of crack growth rate under programmed loading. This behaviour of growth rate results from a plastic zone formed in the front of crack tip and a crack closure effect. However, classical plots of crack growth rates did not confirmed these significant variations. Moreover, the research has proven that under CA loading the crack growth rate does not depend on the direction of specimen's cutting. To the contrary, in the second case of loading (OVL) the results indicate that there is a dependence of the cutting direction on crack growth behaviour, particularly in the range of shorter cracks.

The research was supported by Ministry of Scientific Research and Information Technology, Grant No 7 T07B 004 19.

Manuscript received by Editorial Board, January 12, 2004;
final version, April 27, 2004.

REFERENCES

[1] Kocańda S.: Fatigue Failure of Metals. Sijthoff a. Noordhoff International Publishers, Alphen an den Rijn, 1978.
Kocańda S.: Metal Fatigue. Part III, in Experimental Methods in Mechanics of Solids. Amsterdam-Oxford-New York, Elsevier, 1990, PWN Warszawa, 1990.
Kocańda S.: Fatigue Cracking of Metals. (in Polish – Zmęczeniowe pękanie metali). Wyd. III, WNT Warszawa, 1985.

[2] Kocańda D., Kocańda S., Torzewski J.: Fatigue crack growth rate in 2024-T3 aluminium alloy. Proc. XIX Symposium on Fatigue and Fracture Mechanics (Zmęczenie i Mechanika Pękania, Materiały XIX Sympozjum) Publishing of ATR Bydgoszcz, 2002, pp. 195÷202 (*in Polish*).

[3] Wanhill R. J. H.: Flight simulation fatigue crack growth guidelines, Proc. Eighth Int. Fatigue Congress – Fatigue 2002, Sweden, 2002, Ed.: A. Blom, Vol. 1/5, pp. 573÷584.

[4] Spence S. H., Williams N. M., Stonham A. J., Bache M. R., Ward A. R., Evans W. J., Hay D., Urbani C., Crawford B. R., Loader C., Clark G.: Fatigue in the presence of corrosion pitting in an aerospace aluminium alloy, Ibidem, pp. 701÷708.

[5] Katoh Y., Nakayama H., Tanaka T.: Fatigue crack growth behaviour of aluminium alloy under three-step varying load, Ibidem, Vol. 2/5, pp. 1459÷1466.

[6] Sunder R.: An explanation for the residual stress effect in metal fatigue, Ibidem, Vol. 5/5, pp. 3339÷3350.

[7] Gangloff R. P.: Environment sensitive fatigue crack tip process and propagation in aerospace aluminium alloys, Ibidem, Vol. 5/5, pp. 3401÷3430.

[8] Forth S. C., Keat W. D., Fawrow L. H.: Experimental and computational investigation of three-dimensional mixed-mode fatigue. J. Fatigue Fract. Engng Mater. Struct. 2002, Vol. 25, No 1, pp. 3÷15.
[9] Schijve J.: Fatigue of Structures and Materials. Kluwer Academic Publishers, Dordrecht, Boston, London, 2001.
[10] Schijve J.: Fatigue of structures and materials in the 20th century and the state of the art. Fracture Mechanics Beyond 2000, Proc. 14th Bienniel Conference on Fracture – ECF 14, Cracow, 2002, Ed.: A. Neimitz, I. V. Rokach, D. Kocańda, K. Gołoś, EMAS Publishing, Sheffield, Kielce University of Technology, Vol. II/III, pp. 211÷262.
[11] Zhang X. P., Wang C. H., Ye L., Mai W.: In situ investigation of small fatigue crack growth in poly-crystal and single-crystal aluminium alloys. J. Fatigue Fract. Engng Mater. Struct. 2002, Vol. 25, No 2, pp. 141÷150.
[12] Kermanidis A. T., Pantelakis S. G.: Fatigue crack growth analysis of 2024-T3 aluminium specimens under aircraft service spectra. J. Fatigue Fract. Engng Mater. Struct., 2001, Vol. 24, pp. 699÷710.
[13] Ranganathan N.: Certain aspects of variable amplitude fatigue, Proc. Eighth Int. Fatigue Congress – Fatigue 2002, Sweden, 2002, Ed.: A. Blom, Vol. 1/5, pp. 613÷621.
[14] Brockenbrough J. R., Bucci R. J., Kulak M., Zonker H. R., Bray G. H., Heinimann M. B., Newman J. C.: Crack growth prediction methods for spectrum loading to support fatigue and durability damage tolerance evaluation. Int. Committee on Aeronautical Fatigue (ICAF), Fatigue of Aeronautical Structures as an Engineering Challenge, Lucerne, Switzerland, 2003, p. 14.
[15] Goncalves W., Pramono A., Chaves C. E.: Embraer new family of jets-meeting the current fatigue and damage tolerance requirements. Ibidem, p. 21.
[16] Lazzeri L., Ratti G.: Fatigue crack propagation in thin sheets under typical helicopter spectra, Proc. Eighth Int. Fatigue Congress – Fatigue 2002, Sweden, 2002, Ed.: A. Blom, Vol. 1/5, pp. 585÷592.
[17] Iyyer N. S., Kwon Y. S., Nam Phan: P-3C crack growth life predictions under spectrum loading. International Committee on Aeronautical Fatigue (ICAF), Fatigue of Aeronautical Structures as an Engineering Challenge, Lucerne, Switzerland, 2003, p. 18.
[18] Skorupa M.: Empirical Trends and Prediction Models for Fatigue Crack Growth under Variable Amplitude Loading. Netherlands Energy Research Foundation ECN-R-96-007, 1996.
[19] Dowling N. E.: Mechanical Behavior of Materials. Prentice Hall, New Jersey, 1999.

Rekonstrukcja prędkości zmęczeniowego pękania w stopie aluminium 2024-T3 na podstawie analizy fraktograficznej

Streszczenie

Treścią pracy są badania zmęczeniowego rozwoju pęknięć w próbkach z platerowanych blach ze stopu aluminium 2024-T3 w dwóch stanach obciążeń cyklicznych: przy stałoamplitudowym jednostronnie zmiennym rozciąganiu (R=0.1) (CA) i przy zmiennoamplitudowym rozciąganiu z pojedynczymi i wielokrotnymi przeciążeniami (OVL). Drugi program obciążeń jest stosowany w badaniach symulacyjnych rozwoju pęknięć w skrzydłach statków latających. Badania prowadzono w celu poznania wpływu obciążenia na powstawanie układów prążków zmęczeniowych na powierzchni pęknięć oraz możliwości odtwarzania historii obciążenia na podstawie charakterys-

tycznych cech budowy powierzchni pęknięć. Prędkość zmęczeniowego pękania, określoną na podstawie pomiarów przyrostu długości pęknięć na powierzchni próbek w danym przedziale czasu porównano z prędkością pękania odczytaną z odległości międzyprążkowych na powierzchni pęknięć. Otrzymano dobrą zgodność tych prędkości w przypadku obciążenia stałoamplitudowego. Kierunek wycięcia elementów modelowych względem kierunku walcowania blachy nie wpłynął na ich prędkość pękania, ale zaznaczył się przy obciążeniu OVL. Przy tym obciążeniu porównywano prędkość pękania wzdłuż powierzchni próbek z uśrednioną prędkością pękania obliczoną z odległości międzyprążkowych na powierzchni pęknięć, które odpowiadały poszczególnym blokom obciążeń. Analiza mikrofraktograficzna dowiodła dużej zmienności pękania w obrębie bloków obciążeń. Ujawnione w skali mikroskopowej opóźnianie i przyspieszanie prędkości pękania powiązano z wielkością stref plastycznych na czole pęknięć i z zamykaniem się pęknięcia pod wpływem przeciążeń w widmie OVL.